Atmospheric Environment 75 (2013) 24–31

Contents lists available at SciVerse ScienceDirect

Atmospheric Environment

journal homepage: www.elsevier.com/locate/atmosenv

Ozone and particulate matter enhancements from regional wildfires observed at Mount Bachelor during 2004–2011

N.L. Wigder [a,*], D.A. Jaffe [a,b], F.A. Saketa [b]

[a] Department of Atmospheric Sciences, University of Washington, 408 Atmospheric Sciences-Geophysics Building, Box 351640, Seattle, WA 98195, USA
[b] Science and Technology Program, University of Washington-Bothell, 18115 Campus Way Northeast, Box 358581, Bothell, WA 98011, USA

HIGHLIGHTS

- We report enhancement ratios for 32 wildfires in the western US and Canada.
- We find significant secondary organic aerosol formation in plumes aged <2 days.
- Ozone production may be impacted by the altitude of plume transport.
- The presence of urban emissions enhances ozone production in wildfire plumes.

ARTICLE INFO

Article history:
Received 8 February 2013
Received in revised form
27 March 2013
Accepted 9 April 2013

Keywords:
Wildfire
Enhancement ratio
Ozone
Particulate matter
Plume transport

ABSTRACT

We report observations of normalized enhancement ratios (NER) for 32 wildfires measured at Mount Bachelor Observatory in central Oregon during June–September 2004–2011. All 32 plumes resulted from wildfires originating in the western United States and Canada. The observed NER of PM_1 (particulate matter < 1 micron) to carbon monoxide ($\Delta PM_1/\Delta CO$) ranged from 0.06 to 0.42 μg m^{-3} $ppbv^{-1}$. The NER of ozone to CO ($\Delta O_3/\Delta CO$) ranged from 0.01 to 0.51 ppbv $ppbv^{-1}$ for the 13 observed plumes with a significant $\Delta O_3/\Delta CO$ NER ($p \leq 0.01$, $R^2 \geq 0.30$). For wildfire plumes transported <540 km, or approximately <2 days, the $\Delta PM_1/\Delta CO$ NER is found to increase with increasing distance, suggesting that there is significant secondary organic aerosol (SOA) production in these plumes. However, two plumes transported over greater time periods have relatively low $\Delta PM_1/\Delta CO$ NER, indicating that PM_1 loss is greater than SOA production in these plumes. Of the three plumes transported the longest distance to MBO, only two have significant O_3 production. These two plumes were transported in boundary layer air masses, while the third was transported in a free tropospheric air mass, suggesting that conversion of nitrogen oxides (NO_X) to peroxyacetyl nitrate (PAN) may be a factor affecting O_3 production in these plumes. Two wildfire plumes are mixed with urban emissions from the Seattle/Tacoma metropolitan area, and have relatively higher $\Delta O_3/\Delta CO$ NER than other wildfire plumes transported over similar distances.

1. Introduction

Wildfires are a global source of numerous primary and secondary air pollutants (Akagi et al., 2011; Andreae and Merlet, 2001). Many factors impact the relative proportions of trace gases and aerosols emitted from wildfires and produced during plume transport including fire size, fuel type and loading, fire combustion efficiency and meteorological conditions (Akagi et al., 2011; Jaffe and Wigder, 2012). A number of recent aircraft and in situ studies report fire emissions and downwind mixing ratios of ozone (O_3) and $PM_{2.5}$ (particulate matter < 2.5 microns in diameter) in the western United States (US) and Canada (Akagi et al., 2012; Burling et al., 2011; Hecobian et al., 2011; Jaffe et al., 2008; McKendry et al., 2011; Singh et al., 2012). These results demonstrate large variability

Abbreviations: BC, British Columbia; BL, boundary layer; CA, California; CO, carbon monoxide; EDAS, Eta Data Assimilation System; FIRMS, Fire Information for Resource Management System; FT, free troposphere; GDAS, Global Data Assimilation System; $H_2O(g)$, water vapor; HYSPLIT, Hybrid Single Particle Lagrangian Integrated Trajectory; MBO, Mount Bachelor Observatory; MODIS, Moderate Resolution Imaging Spectroradiometer; MDL, method detection limit; NAAPS, Navy Aerosol Analysis and Prediction System; NER, normalized enhancement ratio; NO_X, nitrogen oxides; OA, organic aerosol; OR, Oregon; O_3, ozone; PAN, peroxyacetyl nitrate; PM_1, particulate matter < 1 micron; $PM_{2.5}$, particulate matter < 2.5 microns; PNW, Pacific Northwest; SOA, secondary organic aerosol; STP, standard temperature and pressure.

* Corresponding author. Tel.: +1 425 352 3495; fax: +1 425 352 5233.
E-mail address: nwigder@uw.edu (N.L. Wigder).

1352-2310/$ – see front matter © 2013 Elsevier Ltd. All rights reserved.
http://dx.doi.org/10.1016/j.atmosenv.2013.04.026

in the emissions and subsequent photochemistry of temperate and boreal fire plumes.

Production of secondary air pollutants, especially O_3 and secondary organic aerosol (SOA), are important to understanding the relative concentrations of these pollutants for the global budget and regional air quality assessments (Akagi et al., 2012). Ozone is created from the interaction of nitrogen oxides (NO_X) and non-methane organic compounds in the presence of sunlight. Wildfire O_3 production is highly variable, although O_3 enhancements in wildfire plumes (relative to carbon monoxide (CO) enhancements) generally increase with increasing plume age. In a recent literature review, Jaffe and Wigder (2012) found that the enhancement ratio of O_3 relative to CO ($\Delta O_3/\Delta CO$) in boreal and temperate wildfires was on average 0.018, 0.15 and 0.22 ppbv ppbv^{-1} for plumes aged 1–2 days, 2–5 days and $\geq$5 days, respectively. Additionally, Real et al. (2007) found that high concentrations of aerosols in wildfire plumes can either decrease or increase net O_3 mixing ratios, as the presence of aerosols affects the rates of both photochemical O_3 production and loss.

The limiting factor in wildfire O_3 production is typically NO_X (Jaffe and Wigder, 2012; Mauzerall et al., 1998; Singh et al., 2012). Mixing ratios of NO_X in fire plumes are impacted by the fire combustion efficiency, fuel nitrogen content, and photochemical production and loss of species such as peroxyacetyl nitrate (PAN). Conversion of NO_X to PAN has been shown to account for a large fraction of rapid NO_X loss in boreal (Alvarado et al., 2010) and temperate (Akagi et al., 2012) fire plumes. Wildfire plumes that are mixed with urban emissions have higher O_3 mixing ratios, partly due to the addition of urban NO_X emissions (Akagi et al., 2013; Singh et al., 2012). Recent studies have also shown that NO_X emissions from wildfires may be enhanced due to deposition of urban emissions prior to the fire ignition (Burling et al., 2011; Yokelson et al., 2011).

Particulate matter (PM) is both a primary and secondary pollutant from wildfires. Approximately 80–90% of particulate aerosol volume in biomass burning emissions is in the accumulation mode (PM_1: PM < 1 micron in diameter; Reid et al., 2005), although many wildfire studies report $PM_{2.5}$ concentrations, which is a measurement used in US and Canadian regulations. A laboratory study of fire-integrated biomass burning emissions showed that $PM_{2.5}$ emission factors depend on both the type of fuel burned and the fire combustion efficiency (McMeeking et al., 2009). The rate of secondary organic aerosol (SOA) production is a major factor affecting the evolution of PM concentrations in wildfire plumes (Akagi et al., 2012). In a recent study of a prescribed chaparral fire in California, Akagi et al. (2012) found that the enhancement of $PM_{2.5}$ (relative to the enhancement of carbon dioxide) did not increase during the first 4–4.5 h of plume aging. Differently, a study of a plume in Mexico as part of the MILAGRO campaign showed that $PM_{2.5}$ concentrations increased by a factor of 2.6 after approximately 1.4 h (Yokelson et al., 2009). The authors also found that the enhancement ratio of black carbon to CO was conserved as the plume aged, but the enhancement ratio of organic aerosols (OA) to CO strongly increased, signaling that the increase in $PM_{2.5}$ is attributable to SOA production. Additionally, in a study of OA data from several aircraft campaigns, Jolleys et al. (2012) found that there was little SOA production in aged biomass burning plumes, although the authors noted a wide variation in measured OA enhancements among studies.

In this study, we analyze the enhancements of PM_1 and O_3 in 32 wildfire plumes observed at Mount Bachelor Observatory (MBO) during June–September 2004–2011. All 32 plumes result from fires in the western US and Canada, allowing us to study the variations in PM_1 and O_3 enhancements from regional wildfires. This study presents the largest dataset of wildfire plumes in the US Pacific Northwest (PNW) to date and is the first comprehensive analysis of wildfire plumes observed at MBO.

2. Methods

2.1. Mount Bachelor Observatory site description and measurements

MBO is a mountaintop site located in central Oregon, US (43.98° N, 121.69°W, 2763 m above sea level) and is well positioned to observe long-range transport of Asian industrial and biomass burning plumes, as well as North American wildfires (Ambrose et al., 2011; Finley et al., 2009; Jaffe et al., 2005; Weiss-Penzias et al., 2007, 2006). During 2004–2011, measurements of CO, submicron aerosol scattering, O_3 and meteorological parameters were taken at MBO during the fire season (June–September). Carbon monoxide was sampled with a Thermo Electron Corporation non-dispersive infrared analyzer and O_3 with a Dasibi UV absorbance instrument (Weiss-Penzias et al., 2006). During 2004–2009 submicron dry aerosol scattering (at 535 nm) was measured with a Radiance Research M903 nephelometer (Weiss-Penzias et al., 2006). Submicron dry aerosol scattering (at 450, 550 and 700 nm) was measured with a TSI Model 3563 nephelometer during 2010–2011 (Fischer et al., 2010), and the 550 nm scattering coefficients are used in this analysis. For consistency, the 550 nm aerosol scattering coefficients were adjusted to 535 nm following the method of Müller et al. (2011). Briefly, this method uses the equation $\sigma_{535} = \sigma_{550}{}^{*}(\lambda_{550}/\lambda_{535})^{\alpha 450,550}$, where σ refers to a scattering coefficient, λ refers to a wavelength and α is the Angstrom Exponent calculated at the two wavelengths specified. Aerosol scattering data was corrected to STP ($T = 273.15$ K, $P = 1013.25$ kPa) and then converted to mass concentrations ($\mu g\ m^{-3}$) using a dry aerosol scattering efficiency of 3.6 $m^2\ g^{-1}$ (Hand and Malm, 2007). This dry aerosol scattering efficiency was used because it was determined to be the best for mixed composition aerosols by the Hand and Malm (2007) review article; however, it should be noted that mass scattering efficiencies have been shown to change as a plume ages (Akagi et al., 2012) and that there are uncertainties in all mass scattering efficiencies. Water vapor ($H_2O(g)$) mixing ratios were calculated from measurements of temperature and relative humidity taken with a Campbell Scientific HM45C. All trace gas, aerosol and meteorological observations analyzed were one-hour averages, and concentrations below the method detection limits (MDL) were set to one-half of the MDL.

2.2. Wildfire identification

Wildfires were identified in the MBO dataset using a combination of PM_1 and CO observations, satellite data and trajectory models. First, potential fire time periods were identified based on three criteria: (1) PM_1 and CO concentrations were elevated above the background, (2) for at least one hour, ambient aerosol scattering $\geq$ 20 Mm^{-1} and CO $\geq$ 125 ppbv, and (3) there was a strong correlation ($R^2 \geq 0.70$) between the aerosol scattering and CO observations. Next, Hybrid Single Particle Lagrangian Integrated Trajectory (HYSPLIT) model backward air mass trajectories were initiated from MBO at intervals throughout each of the potential fire periods (Draxler, 1999; Draxler and Hess, 1997, 1998). Both 10-day backward trajectories using the 1° resolution Global Data Assimilation System (GDAS) meteorological data and 3-day backward trajectories using the 40 km resolution US Eta Data Assimilation System (EDAS) meteorological data were calculated. Finally, several satellite products and models were used to identify fires or fire plumes intersecting the calculated trajectory paths. These products were:

- The FIRMS Web Fire Mapper (http://firms.modaps.eosdis.nasa.gov/firemap), which maps fire pixels that are identified using the MODIS instruments on the Aqua and Terra satellites. Only high confidence fire pixels (confidence $\geq$ 80%) were considered.
- MODIS Near Real Time (Orbit Swath) Images (http://lance-modis.eosdis.nasa.gov/cgi-bin/imagery/realtime.cgi) from the Aqua and Terra satellites.
- The Navy Aerosol Analysis and Prediction System (NAAPS) global aerosol model (http://www.nrlmry.navy.mil/aerosol/).

For all fires considered in this analysis, one or more of the sources above showed a fire pixel or plume intersecting the calculated backward air mass trajectories during the fire time period, and for the majority of the fires analyzed, a cloud-free MODIS image of the smoke plume was available. It should be noted that the uncertainties in this source identification technique include errors in modeled data, errors in satellite retrievals of fire pixels due to fire size, lifetime and plume injection height, and the uncertainties associated with using trajectories when plume injection heights are not known. However, the resources listed above were also consulted for at least one day preceding and following each fire event to increase the likelihood of identifying the correct source of each wildfire plume.

Figs. 1 and 2 show an example of this method for a wildfire observed at MBO on 14–15 September 2008. Fig. 1a shows the time series of CO, PM_1 and O_3 observations at MBO for this event, and Fig. 1b and c show reduced major axis fits for PM_1 and O_3 data with the CO data. Fig. 2 shows the mean and total area covered by 24-h backward HYSPLIT trajectories initiated at MBO every hour during the event, combined with MODIS Terra satellite images and MODIS Aqua and Terra fire pixels on 14 September 2008.

2.3. Normalized enhancement ratios

For all identified fires, we calculated normalized enhancement ratios (NER) of PM_1 to CO ($\Delta PM_1/\Delta CO$, $\mu g\ m^{-3}\ ppbv^{-1}$) and O_3 to CO ($\Delta O_3/\Delta CO$, ppbv $ppbv^{-1}$). This method for calculating NERs assumes that the pollutants are co-emitted and that CO is non-reactive (Akagi et al., 2011). The NER for each fire was calculated using hourly data points for the fire time period plus five hourly data points before and after this period. The NER is the slope of a reduced major axis regression of the two variables. As an example, the slopes shown in Fig. 1 are reported as NER for wildfire #22 in Table 1.

2.4. Fire plume categorization by boundary layer/free troposphere influence

There is generally a diurnal cycle in water vapor ($H_2O(g)$) mixing ratios at MBO, with higher mixing ratios in the daytime when upslope flow of boundary layer (BL) air masses predominates and lower mixing ratios at night when downslope flow of free tropospheric (FT) air masses predominates (Weiss-Penzias et al., 2006). Ambrose et al. (2011) showed that water vapor mixing ratios observed at MBO can be used to distinguish FT and BL air masses at the site. Therefore, we calculated water vapor enhancements ($\Delta H_2O(g)$) for each fire plume and used these to identify whether the polluted air mass descended to MBO from the FT or ascended to MBO from the BL.

To calculate the $\Delta H_2O(g)$ for each fire plume, we first identified the hour when the highest CO mixing ratio was observed at MBO, which would indicate the peak of the fire influence. The $\Delta H_2O(g)$ for the plume was defined as the monthly mean $H_2O(g)$ mixing ratio subtracted from the observed $H_2O(g)$ mixing ratio at this hour.

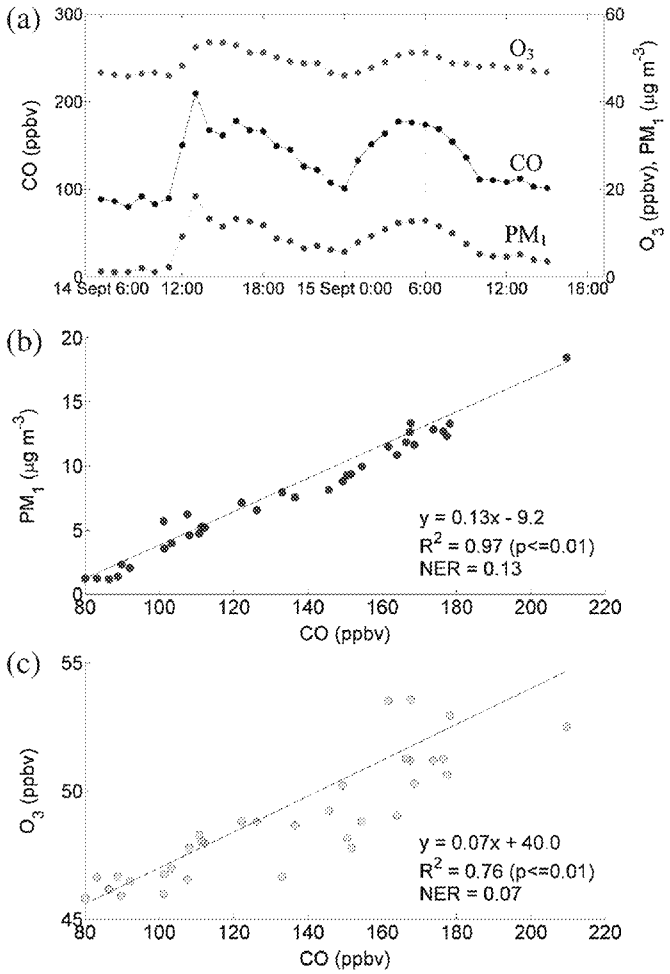

Fig. 1. Time series of CO, PM_1 and O_3 observations at MBO for fire event #22, 14–15 September 2008 (a), and reduced major axis correlations between these PM_1 and CO data (b) and O_3 and CO data (c).

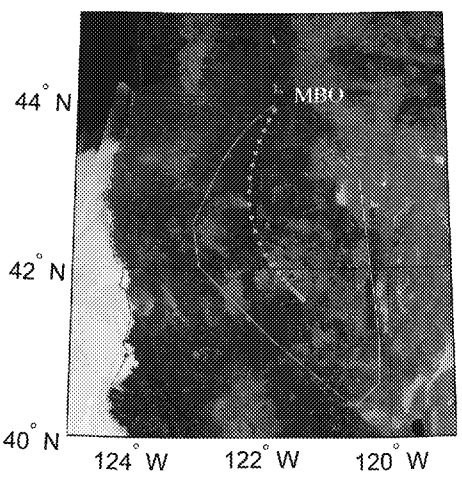

Fig. 2. Evidence for the source of fire event #22, 14–15 September 2008, including the mean of 24-h backward HYSPLIT trajectories initiated at MBO every hour during the event (dotted line), the total area covered by these hourly backward trajectories (solid line), MODIS Aqua and Terra fire pixels with $\geq$80% confidence for 14 September 2008 (red dots), and MODIS Terra satellite images for 14 September 2008. The wildfire source was identified as the fire pixel intersecting the dotted line. (For interpretation of the references to color in this figure legend, the reader is referred to the web version of this article.)

Table 1
Identified wildfire plumes at MBO during 2004–2011.

Event number	Date and time (UTC) when plume observed at MBO	$\Delta PM_1/\Delta CO$ ($\mu g\ m^{-3}\ ppbv^{-1}$)	Distance category or approximate fire location[a]	Time of peak CO (UTC)	$\Delta H_2O(g)$ ($g\ kg^{-1}$)	Air mass source at peak time[b]	$\Delta O_3/\Delta CO$ ($ppbv\ ppbv^{-1}$)
1[c]	28 Jul 2:00–29 Jul 3:00, 2004	0.21	1	4:00	1.79	BL	0.17
2	14 Aug 10:00–18:00, 2004	0.19	4	11:00	−0.07		0.05
3	16 Aug 14:00–17 Aug 21:00, 2004	0.17	1	17:00 (17 Aug)	0.89	BL	
4[c]	19 Aug 9:00–17:00, 2004	0.19	1	14:00	1.05	BL	0.38
5	20 Aug 0:00–11:00, 2004	0.21	Central Oregon (OR)/BC	8:00	2.37	BL	0.51
6	10 Jul 13:00–20:00, 2007	0.29	2	16:00	−1.84	FT	
7	11 Jul 1:00–15:00, 2007	0.21	2	13:00	−0.99	FT	0.19
8	15 Jul 5:00–17 Jul 22:00, 2007	0.27	3	7:00 (16 Jul)	2.04	BL	
9	2 Aug 19:00–3 Aug 2:00, 2007	0.12	Eastern OR/western Montana	21:00	1.79	BL	0.11
10	11 Aug 9:00–16:00, 2007	0.18	1	15:00	−0.67	FT	
11	14 Aug 2:00–9:00, 2007	0.23	1	4:00	1.34	BL	
12	30 Jun 6:00–4 Jul 15:00, 2008	0.23	Northern CA	18:00 (3 Jul)	4.20	BL	0.14
13	15 Jul 17:00–16 Jul 16:00, 2008	0.19	3	5:00	2.20	BL	0.19
14	19 Jul 22:00–22 Jul 16:00, 2008	0.29	3	17:00 (20 Jul)	−0.75	FT	
15	24 Jul 19:00–26 Jul 3:00, 2008	0.30	2	23:00 (25 Jul)	2.65	BL	
16	27 Jul 7:00–14:00, 2008	0.29	2	10:00	1.34	BL	
17	28 Jul 19:00–29 Jul 14:00, 2008	0.28	2	3:00	1.52	BL	0.21
18	31 Jul 10:00–16:00, 2008	0.24	2	12:00	0.95	BL	
19	4 Aug 5:00–5 Aug 5:00, 2008	0.30	3	20:00	0.12		0.14
20	7 Aug 22:00–9 Aug 6:00, 2008	0.33	3	7:00	1.10	BL	0.07
21	17 Aug 5:00–11:00, 2008	0.19	Central Oregon/northern CA	8:00	1.49	BL	
22	14 Sep 11:00–15 Sep 10:00, 2008	0.13	1	13:00	−0.50	FT	0.07
23	17 Sep 13:00–18 Sep 6:00, 2008	0.16	1	16:00	0.12		0.01
24	24 Sep 1:00–26 Sep 1:00, 2008	0.14	Southwestern OR/northern CA	4:00 (25 Sep)	1.02	BL	
25	26 Sep 19:00–27 Sep 4:00, 2008	0.11	Southwestern OR/northern CA	2:00	0.61	BL	
26	16 Sep 15:00–17 Sep 5:00, 2009	0.15	1	21:00	2.65	BL	
27	18 Sep 19:00–19 Sep 12:00, 2009	0.16	1	4:00	1.12	BL	
28	22 Sep 9:00–15:00, 2009	0.42	Southern/eastern OR	13:00	−2.63	FT	
29	23 Sep 21:00–25 Sep 14:00, 2009	0.26	1	11:00 (24 Sep)	−1.02	FT	
30	28 Sep 3:00–23:00, 2009	0.17	1	5:00	−0.62	FT	
31	1 Aug 8:00–2 Aug 19:00, 2010	0.10	5	13:00 (1 Aug)	−2.20	FT	
32	5 Aug 4:00–8 Aug 3:00, 2010	0.22	1	9:00 (5 Aug)	0.21		

[a] Distance category (from MBO; Section 3.1) only listed for events with wildfire emissions resulting from a localized area (Section 3). For all other events, the approximate locations of wildfires contributing to the observed plume are listed. 1: <140 km; 2: 140–340 km; 3: 340–540 km; 4: 540–740 km; 5: >740 km.
[b] Air mass sources assigned using $\Delta H_2O(g)$ (Section 3.2). No source defined for $\Delta H_2O(g)$ between −0.50 and 0.50. BL: boundary layer; FT: free troposphere.
[c] These events are identified as mixed wildfire and urban emissions.

A negative $\Delta H_2O(g)$ indicates that the air mass was relatively dry and likely descending from the FT and a positive $\Delta H_2O(g)$ indicates that it was ascending from the BL. To account for error in the $\Delta H_2O(g)$ calculation, plumes with $\Delta H_2O(g)$ between −0.50 and 0.50 were not considered a member of either category.

This method for distinguishing BL and FT air masses at MBO assumes that the $H_2O(g)$ emissions from wildfires are negligible when compared to the $H_2O(g)$ mixing ratios of the air masses carrying the wildfire pollutants. To test this assumption, we used the laboratory biomass burning emissions from Yokelson et al. (1996) to estimate the $H_2O(g)$ emissions for common wildfire fuels. First, we calculated the $\Delta H_2O(g)/\Delta CO$ ($g\ kg^{-1}\ ppbv^{-1}$) for these fuels using the Yokelson et al. (1996) emission factors and assuming $T = 298$ K and $P = 733$ hPa. These assumptions are based on summertime MBO data. The calculated $\Delta H_2O(g)/\Delta CO$ for the fuels ranged from 7.2×10^{-6} to 3.4×10^{-5} $g\ kg^{-1}\ ppbv^{-1}$. The maximum observed wildfire ΔCO at MBO during 2004–2011 was approximately 2700 ppbv, giving a $\Delta H_2O(g)$ of 0.02–0.09 $g\ kg^{-1}$. Given that this range is at least two orders of magnitude smaller than the average $\Delta H_2O(g)$ in both FT and BL air masses (Table 1), we can safely assume that $H_2O(g)$ emissions from wildfires are negligible in our analysis, and did not affect our method for distinguishing BL and FT air masses.

3. Results and discussion

This analysis identified 32 wildfire plumes observed at MBO during June–September 2004–2011 (Table 1, Fig. 3). The sources of all these plumes were wildfires in the western United States and

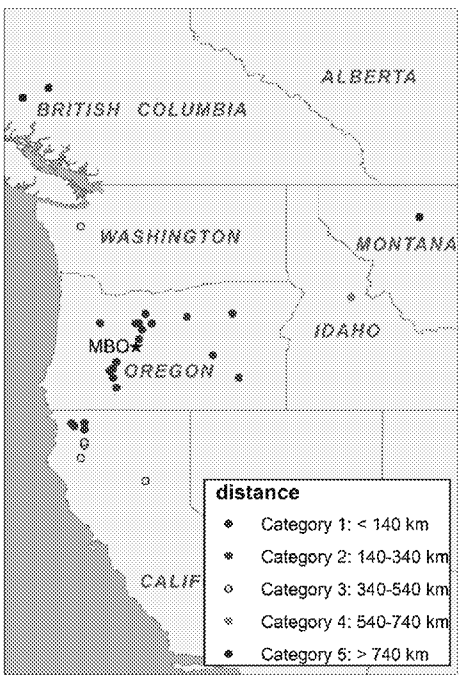

Fig. 3. Approximate source locations of wildfire plumes observed at MBO. Colors represent the Euclidian distance of the fire source from MBO. Note that some of the plumes in Table 1 mix emissions from two or more fire locations, and are therefore represented by more than one point on this map. (For interpretation of the references to color in this figure legend, the reader is referred to the web version of this article.)

Canada. Finley et al. (2009) previously reported observations of particulate and gaseous mercury associated with the 2007 fires, and Weiss-Penzias et al. (2007) reported NER for ten fires observed at MBO during 2004–2005. Some of the Weiss-Penzias et al. (2007) and Finley et al. (2009) fire events are also included in this analysis and others are not because they did not meet the criteria listed in Section 2.2. It should be noted that the lack of wildfires identified in 2005, 2006 and 2011 is due to maintenance on the CO and/or aerosol scattering instruments during the majority of the fire season in these years.

Each plume was defined as originating from a localized area or from multiple areas. For plumes defined as originating from a localized area, the backward air mass trajectories crossed only one group of MODIS fire pixels. A group of fire pixels was defined as two or more pixels no more than 75 km from each other. This distance was chosen because analysis of MODIS orbit swath images showed that smoke from fire pixels at this distance often mixed, resulting in one fire plume rather than individual plumes for each fire pixel. For plumes defined as originating from multiple areas, the backward air mass trajectories crossed more than one group of fire pixels. Of the 32 plumes identified, 25 originated from a localized area, and two of these were likely mixed with urban pollution from the Seattle/Tacoma metropolitan area (Table 1).

3.1. Particulate matter enhancement ratios

The $\Delta PM_1/\Delta CO$ NER of the wildfire plumes observed at MBO ranged from 0.06 to 0.42 $\mu g\ m^{-3}\ ppbv^{-1}$ (Table 1). Of the 32 plumes identified, 23 originated from a localized area and were not mixed with urban emissions (see Section 3). Fig. 3 maps the locations of the wildfires, categorized into five groups by Euclidian distance from MBO. The standard deviation method for classifying spatial data (de Smith et al., 2013) was used to define the groups. Briefly, this method defines categories of data based on standard deviations from the mean. The five defined categories for this analysis (categories 1–5) represent Euclidian distances from MBO of <140, 140–340, 340–540, 540–740, and >740 km, respectively. Using HYSPLIT trajectories, the approximate transport times between the fire source and MBO increases from category 1 to category 5. In general, categories 1–2 represent transport within 1 day, category 3 represents 1–2 days of transport, and categories 4–5 represent more than 2 days of transport. The median $\Delta PM_1/\Delta CO$ NER of wildfire plumes in categories 1–5 is 0.17, 0.29, 0.29, 0.19 and 0.06 $\mu g\ m^{-3}\ ppbv^{-1}$, respectively, although categories 4 and 5 contain only one data point each.

Akagi et al. (2011) reviewed emission factors for biomass burning and found that in temperate regions, average biomass burning emissions per kg of vegetation burned are $89 \pm 32\ g\ kg^{-1}$ for CO and $12.7 \pm 7.5\ g\ kg^{-1}$ for PM measured by instruments with size cuts between 1 and 5 μm. This PM emission factor is similar to the $13.0 \pm 7.0\ g\ kg^{-1}$ $PM_{2.5}$ emission factor calculated by Andreae and Merlet (2001) for extratropical forests. Given this information and the fact that the majority of particulate biomass burning emissions are in the accumulation mode (Reid et al., 2005), we can assume that the Akagi et al. (2011) emission factor for PM is a reasonable estimate for a PM_1 emission factor, even though it combines studies with larger PM size cuts. Assuming $P = 1013.25$ kPa and $T = 298$ K for the conversion of CO to ppbv, the Akagi et al. (2011) data results in a $\Delta PM/\Delta CO$ emission factor ratio of $0.16 \pm 0.11\ \mu g\ m^{-3}\ ppbv^{-1}$ for temperate regions. This large variation in the $\Delta PM/\Delta CO$ emission factor is consistent with a recent wildfire study that showed large variability in plume $\Delta OA/\Delta CO$, even from wildfires in the same biome (Jolleys et al., 2012).

Fig. 4 compares the categorized $\Delta PM_1/\Delta CO$ NER from this study with the temperate $\Delta PM/\Delta CO$ emission ratios from Akagi et al. (2011), the $\Delta PM_{2.5}/\Delta CO$ emission ratio and downwind NER for a single fire plume documented by Akagi et al. (2012), and the $\Delta PM_1/\Delta CO$ NER from Weiss-Penzias et al. (2007). The $\Delta PM/\Delta CO$ for Akagi

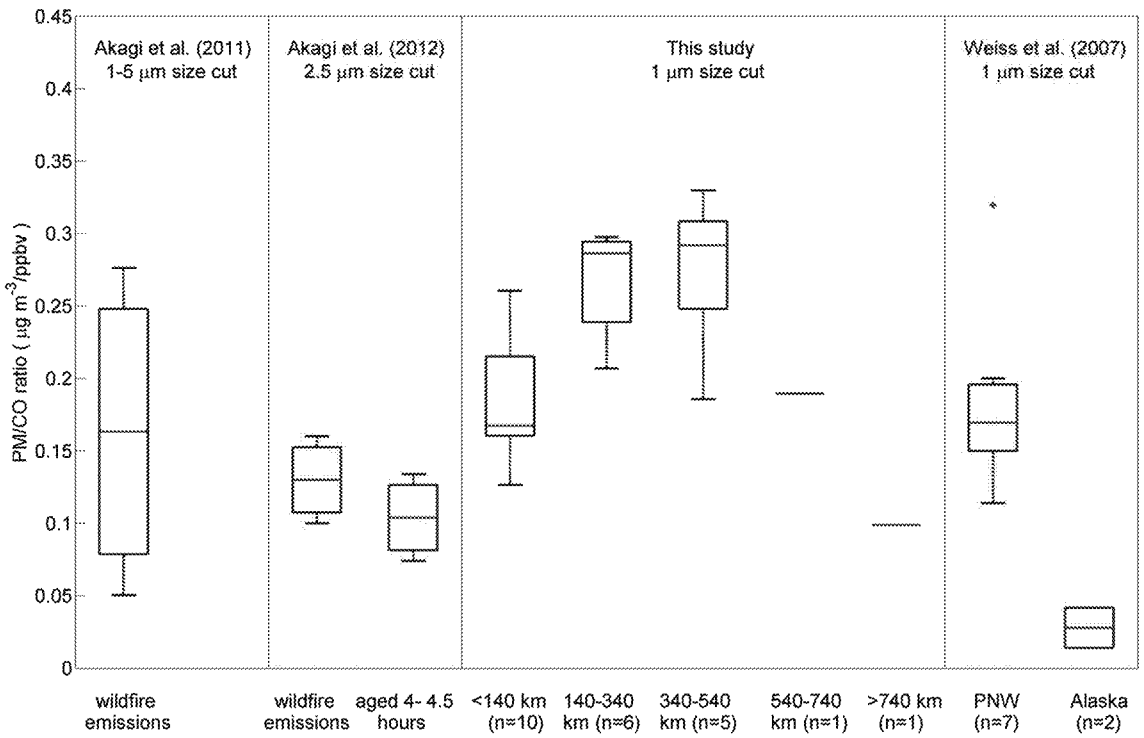

Fig. 4. PM/CO wildfire emission and enhancement ratios. In the box plots, the red line indicates the median, the box delineates the 25th–75th percentile range and red plusses indicate outliers more than twice the interquartile range. Note that the Akagi et al. (2012) 'aged 4–4.5 h' data equals the 'wildfire emissions' from that study multiplied by 0.80 (personal communication with R. Yokelson, 2013). (For interpretation of the references to color in this figure legend, the reader is referred to the web version of this article.)

et al. (2011) and Akagi et al. (2012) were calculated from the emission factors and NER provided in the studies, with the assumption that $P = 1013.25$ kPa and $T = 298$ K for the conversion of CO to ppbv. A dry aerosol scattering efficiency of 3.6 $m^2\ g^{-1}$ was used to convert the Weiss-Penzias et al. (2007) data to mass ratios (see Section 2.1). Akagi et al. (2011) found an average $\Delta PM/\Delta CO$ emission factor ratio of 0.16 ± 0.11 $\mu g\ m^{-3}\ ppbv^{-1}$ for temperate regions. Fig. 4 shows that for category 1 in this study, the median NER approximates the median emission factor from Akagi et al. (2011), demonstrating that SOA production was minimal, or balanced with PM loss, for these plumes transported < 140 km. This result for PNW fires is similar to the results of Akagi et al. (2012) for a California chaparral fire, where the authors found an overall decrease in $\Delta OA/\Delta CO$ during the first four hours of plume aging, indicating that $PM_{2.5}$ concentrations did not increase over this time period (Fig. 4). The median $\Delta PM_1/\Delta CO$ NER for this study increases between categories 1–3, suggesting that SOA production was a dominant factor influencing $\Delta PM_1/\Delta CO$ NER for plumes transported 140–540 km or approximately 0.5–2 days. Only two of the plumes analyzed were transported over greater distances and time (categories 4–5). These two data points show relatively low $\Delta PM_1/\Delta CO$ NER, suggesting that net SOA production during transport was less than net PM_1 loss through deposition, evaporation and/or cloud processing.

The $\Delta PM_1/\Delta CO$ NER from this study are similar to the results of Weiss-Penzias et al. (2007), a study that documented fire events observed at MBO during 2004–2005. The exact locations of the Weiss-Penzias et al. (2007) fires are not known, but the PNW fires would likely fall in categories 1–3 in this study and the Alaska fires would be category 5. Fig. 4 shows that the majority of the Weiss-Penzias et al. (2007) PNW fires have similar $\Delta PM_1/\Delta CO$ NER to category 1 (<140 km) plumes and the Alaska fires have $\Delta PM_1/\Delta CO$ NER slightly lower than the single category 5 (>740 km) plume. Therefore, the Weiss-Penzias et al. (2007) results corroborate our finding that $\Delta PM_1/\Delta CO$ NER is relatively lower for fire emissions transported longer distances.

3.2. Ozone and water vapor enhancements

The $\Delta O_3/\Delta CO$ NER was significant ($p \leq 0.01$, $R^2 \geq 0.30$) for 13 out of 32, or 41%, of the wildfire plumes observed at MBO (Table 1). As shown in Table 1, plumes with significant O_3 enhancements originated from fires at various distances from MBO, including fires in the closest distance categories and fires as far away as British Columbia and Montana. All of the significant $\Delta O_3/\Delta CO$ NER had positive correlations. The O_3 enhancements listed in Table 1 are highly variable but in line with other observations in temperate and boreal regions (Jaffe and Wigder, 2012).

As described in section 2.4, each of the 32 plumes was categorized based on the calculated $\Delta H_2O(g)$ at the time when CO mixing ratios peaked. Table 1 and Fig. 5 show that 19 of the 32 plumes arrived at MBO in BL air masses. Nine of the plumes arrived at MBO in FT air masses, mostly between the hours of 11:00–17:00 UTC (3:00–9:00 local standard time). Fire emissions arriving in BL air masses had peak CO mixing ratios at all hours of the day and night, indicating that time of day alone is not a good indicator of BL air flow during the summer fire season at MBO.

Of the 13 plumes with significant O_3 production, 8 were transported in the BL immediately before reaching MBO and 2 were carried by air masses descending from the FT (Table 1). The remaining 3 plumes could not be categorized because of a $\Delta H_2O(g)$ close to zero. The two plumes with significant O_3 production that are categorized as FT air masses are in distance categories 1 and 2, indicating that the wildfire pollutants were transported to MBO within one day (Section 3.1). HYSPLIT backward trajectories for

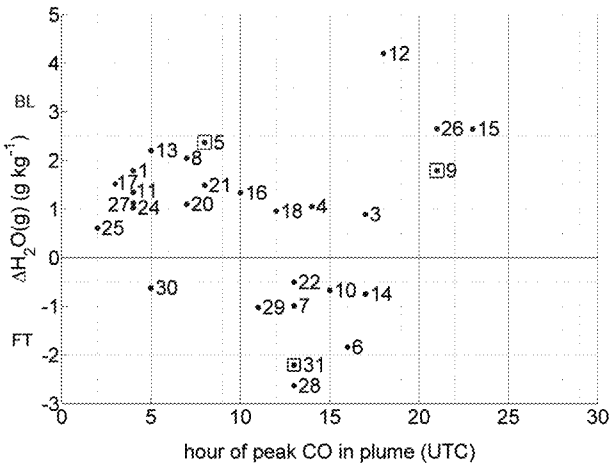

Fig. 5. Fire plume $\Delta H_2O(g)$ versus the hour that the peak CO was observed at MBO, with plume numbers corresponding to Table 1. Blue points symbolize plumes ascending to MBO from the boundary layer and black points represent plumes descending to the site from the free troposphere. Plumes with $\Delta H_2O(g)$ between −0.50 and 0.50 are not categorized. Squares mark fires 5, 9 and 31. (For interpretation of the references to color in this figure legend, the reader is referred to the web version of this article.)

these two events show that the air masses did descend from high in the free troposphere. However, the trajectories also show that within the last 24 h before reaching MBO, the air masses for both events were transported approximately at or lower than the altitude of MBO, and crossed above identified fire hotspots. Therefore, it is realistic to assume that the fire emissions were injected into the air masses during these last 24 h of transport before reaching MBO. This suggests that O_3 in these plumes was either produced at the fire location or during the relatively low-altitude transport to MBO, rather than being produced from fire emissions lofted high into the upper free troposphere.

In general O_3 production increases over time (Jaffe and Wigder, 2012), so we would expect significant O_3 production in the wildfire plumes that were transported the longest. The three wildfire plumes analyzed that included pollutants transported over the greatest distances and time were events 5, 9 and 31 (Table 1). Events 5 and 9 mixed local fire emissions with fire emissions from British Columbia (BC) and Montana, respectively. The source of event 31 was also BC. Events 5 and 9 were classified as arriving at MBO in BL air masses, while event 31 arrived in an FT air mass. Fig. 6 presents the mean height of 48-h HYSPLIT backward trajectories started every hour during events 5, 9 and 31. This figure corroborates the $\Delta H_2O(g)$ classification system, by showing that event 31 descends into MBO from higher altitudes, while events 5 and 9 are

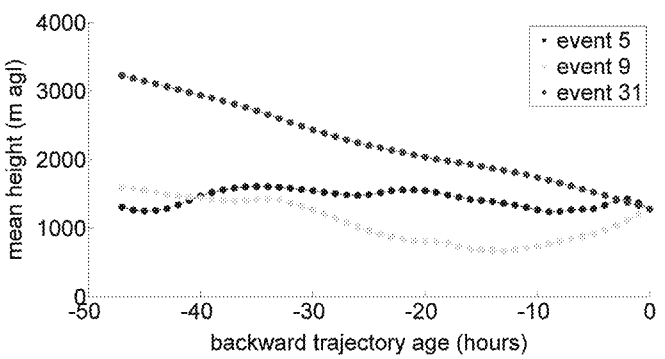

Fig. 6. Mean height for 48-h HYSPLIT backward trajectories initiated at MBO every hour during events 5, 9 and 31.

transported closer to the surface. It is interesting to note that events 5 and 9 were characterized by significant O_3 production, while event 31 was not. This suggests that there may be a difference in the photochemical reactions in plumes transported in the BL compared to those transported in the FT that impacts O_3 production, and that transport distance by itself may not be an adequate indicator of O_3 production.

3.3. Ozone enhancements in wildfire plumes mixed with urban emissions

Two of the identified wildfire plumes were likely mixed with urban emissions from the Seattle/Tacoma metropolitan area. As shown in Table 1, both of these plumes had significantly higher $\Delta O_3/\Delta CO$ NER (0.17, 0.38 ppbv ppbv^{-1}) than the other plumes in the same distance category (0.01, 0.07 ppbv ppbv^{-1}). Akagi et al. (2013) and Singh et al. (2012) also found significantly higher O_3 production in fire plumes mixed with urban emissions, which the studies attributed to higher mixing ratios of NO_X produced in urban areas. It is not clear how the $\Delta O_3/\Delta CO$ NER for a pure Seattle/Tacoma urban plume would compare with the $\Delta O_3/\Delta CO$ NER for this mixed plume, as no such plume has been documented at MBO. However, the analysis of Singh et al. (2012) shows that the range of $\Delta O_3/\Delta CO$ NER for pure urban plumes compared with mixed urban/fire plumes is highly variable, and likely depends on the mixing ratio of NO_X within the plume.

4. Conclusions

We report observations of $\Delta PM_1/\Delta CO$ and $\Delta O_3/\Delta CO$ NER for 32 large wildfire plumes observed at MBO during June–September 2004–2011. For wildfire plumes transported <540 km, or approximately <2 days, greater transport distance yielded higher $\Delta PM1/\Delta CO$ NER, likely due to SOA production. However, two observed plumes transported >540 km, or >2 days, demonstrate relatively low $\Delta PM_1/\Delta CO$ NER. This indicates that net SOA production in these plumes was less than PM_1 loss from wet and dry deposition, cloud processing and/or evaporation. Previous studies of O_3 production from wildfires have found a wide variation in $\Delta O_3/\Delta CO$ NER for plumes transported 1–5 days, with NER ranging from negative to positive values, and with no significant $\Delta O_3/\Delta CO$ NER in some plumes transported over short time periods (Jaffe and Wigder, 2012). Similarly, this study found significant $\Delta O_3/\Delta CO$ NER for only 41% of the wildfire plumes identified, most of which were transported < 2 days before reaching MBO. This differs from wildfire plumes transported over greater time periods, where there is almost always significant O_3 production (Jaffe and Wigder, 2012). For the wildfire plumes analyzed in this study, there was no relationship between distance or time transported and the degree of O_3 production, indicating that multiple factors must explain O_3 production in these plumes transported over relatively short time periods. Similar to the findings of Akagi et al. (2013) and Singh et al. (2012), this analysis found relatively larger $\Delta O_3/\Delta CO$ NER for wildfire plumes mixed with urban emissions.

We used calculations of $\Delta H_2O(g)$ to identify whether each wildfire plume was carried by an air mass descending to MBO from the FT or ascending to MBO from the BL, and this categorization was used to examine three plumes that were transported over relatively long distances to MBO. One of these three plumes descended to MBO in an FT air mass, while the other two were transported in BL air masses. We expect that plumes transported over longer distances are more likely to have significant O_3 production, but only the two plumes transported in the BL had this characteristic. Recent studies have shown that NO_X can be rapidly converted to PAN in temperate and boreal fire plumes (Akagi et al., 2012; Alvarado et al., 2010). PAN will decompose to NO_X as an air mass warms, which can occur as an air mass descends in the atmosphere. It is possible that there was not significant O_3 production in the plume carried in the FT because the majority of the plume nitrogen was in the form of PAN, and the air mass did not reach a high enough temperature during descent for significant PAN decomposition. Overall, this study points toward large variability in wildfire emissions and photochemistry, even within a single biome.

Acknowledgments

Funding for research at MBO was provided by the National Science Foundation (NSF), grant number AGS-1066032AM01. This material is based upon work supported by the NSF Graduate Research Fellowship under grant number DGE-0718124.

References

Akagi, S.K., Yokelson, R.J., Burling, I.R., Meinardi, S., Simpson, I., Blake, D.R., McMeeking, G.R., Sullivan, A., Lee, T., Kreidenweis, S., Urbanski, S., Reardon, J., Griffith, D.W.T., Johnson, T.J., Weise, D.R., 2013. Measurements of reactive trace gases and variable O_3 formation rates in some South Carolina biomass burning plumes. Atmospheric Chemistry and Physics 13, 1141–1165.

Akagi, S.K., Craven, J.S., Taylor, J.W., McMeeking, G.R., Yokelson, R.J., Burling, I.R., Urbanski, S.P., Wold, C.E., Seinfeld, J.H., Coe, H., Alvarado, M.J., Weise, D.R., 2012. Evolution of trace gases and particles emitted by a chaparral fire in California. Atmospheric Chemistry and Physics 12, 1397–1421.

Akagi, S.K., Yokelson, R.J., Wiedinmyer, C., Alvarado, M.J., Reid, J.S., Karl, T., Crounse, J.D., Wennberg, P.O., 2011. Emission factors for open and domestic biomass burning for use in atmospheric models. Atmospheric Chemistry and Physics 11, 4039–4072.

Alvarado, M.J., Logan, J.A., Mao, J., Apel, E., Riemer, D., Blake, D., Cohen, R.C., Min, K.E., Perring, A.E., Browne, E.C., Wooldridge, P.J., Diskin, G.S., Sachse, G.W., Fuelberg, H., Sessions, W.R., Harrigan, D.L., Huey, G., Liao, J., Case-Hanks, A., Jimenez, J.L., Cubison, M.J., Vay, S.A., Weinheimer, A.J., Knapp, D.J., Montzka, D.D., Flocke, F.M., Pollack, I.B., Wennberg, P.O., Kurten, A., Crounse, J., Clair, J.M.S., Wisthaler, A., Mikoviny, T., Yantosca, R.M., Carouge, C.C., Le Sager, P., 2010. Nitrogen oxides and PAN in plumes from boreal fires during ARCTAS-B and their impact on ozone: an integrated analysis of aircraft and satellite observations. Atmospheric Chemistry and Physics 10, 9739–9760.

Ambrose, J.L., Reidmiller, D.R., Jaffe, D.A., 2011. Causes of high O(3) in the lower free troposphere over the Pacific Northwest as observed at the Mt. Bachelor Observatory. Atmospheric Environment 45, 5302–5315.

Andreae, M.O., Merlet, P., 2001. Emission of trace gases and aerosols from biomass burning. Global Biogeochemical Cycles 15, 955–966.

Burling, I.R., Yokelson, R.J., Akagi, S.K., Urbanski, S.P., Wold, C.E., Griffith, D.W.T., Johnson, T.J., Reardon, J., Weise, D.R., 2011. Airborne and ground-based measurements of the trace gases and particles emitted by prescribed fires in the United States. Atmospheric Chemistry and Physics 11, 12197–12216.

de Smith, M., Goodchild, M.F., Longley, P.A., 2013. Geospatial Analysis: a Comprehensive Guide to Principles, Techniques and Software Tools, fourth ed. The Winchelsea Press, Winchelsea, UK. http://www.spatialanalysisonline.com/HTML/index.html (accessed 4.1.13.).

Draxler, R.R., 1999. HYSPLIT4 User's Guide, NOAA Technical Memo ERL ARL-230. NOAA Air Resources Laboratory, Silver Spring, MD.

Draxler, R.R., Hess, G.D., 1998. An overview of the HYSPLIT_4 modeling system of trajectories, dispersion, and deposition. Australian Meteorological Magazine 47, 295–308.

Draxler, R.R., Hess, G.D., 1997. Description of the HYSPLIT_4 Modeling System, NOAA Technical Memo ERL ARL-224. NOAA Air Resources Laboratory, Silver Spring, MD, p. 24.

Finley, B.D., Swartzendruber, P.C., Jaffe, D.A., 2009. Particulate mercury emissions in regional wildfire plumes observed at the Mount Bachelor Observatory. Atmospheric Environment 43, 6074–6083.

Fischer, E.V., Jaffe, D.A., Marley, N.A., Gaffney, J.S., Marchany-Rivera, A., 2010. Optical properties of aged Asian aerosols observed over the U.S. Pacific Northwest. Journal of Geophysical Research 115, D20209.

Hand, J.L., Malm, W.C., 2007. Review of aerosol mass scattering efficiencies from ground-based measurements since 1990. Journal of Geophysical Research 112, D16203.

Hecobian, A., Liu, Z., Hennigan, C.J., Huey, L.G., Jimenez, J.L., Cubison, M.J., Vay, S., Diskin, G.S., Sachse, G.W., Wisthaler, A., Mikoviny, T., Weinheimer, A.J., Liao, J., Knapp, D.J., Wennberg, P.O., Kürten, A., Crounse, J.D., Clair, J.S., Wang, Y., Weber, R.J., 2011. Comparison of chemical characteristics of 495 biomass burning plumes intercepted by the NASA DC-8 aircraft during the ARCTAS/CARB-2008 field campaign. Atmospheric Chemistry and Physics 11, 13325–13337.

Jaffe, D., Chand, D., Hafner, W., Westerling, A., Spracklen, D., 2008. Influence of fires on O_3 concentrations in the western US. Environmental Science & Technology 42, 5885–5891.

Jaffe, D., Prestbo, E., Swartzendruber, P., Weiss-Penzias, P., Kato, S., Takami, A., Hatakeyama, S., Kajii, Y., 2005. Export of atmospheric mercury from Asia. Atmospheric Environment 39, 3029–3038.

Jaffe, D.A., Wigder, N.L., 2012. Ozone production from wildfires: a critical review. Atmospheric Environment 51, 1–10.

Jolleys, M.D., Coe, H., McFiggans, G., Capes, G., Allan, J.D., Crosier, J., Williams, P.I., Allen, G., Bower, K.N., Jimenez, J.L., Russell, L.M., Grutter, M., Baumgardner, D., 2012. Characterizing the aging of biomass burning organic aerosol by use of mixing ratios: a meta-analysis of four regions. Environmental Science & Technology 46, 13093–13102.

Mauzerall, D.L., Logan, J.A., Jacob, D.J., Anderson, B.E., Blake, D.R., Bradshaw, J.D., Heikes, B., Sachse, G.W., Singh, H., Talbot, B., 1998. Photochemistry in biomass burning plumes and implications for tropospheric ozone over the tropical South Atlantic. Journal of Geophysical Research 103, 8401–8423.

McKendry, I., Strawbridge, K., Karumudi, M.L., O'Neill, N., Macdonald, A.M., Leaitch, R., Jaffe, D., Cottle, P., Sharma, S., Sheridan, P., Ogren, J., 2011. Californian forest fire plumes over Southwestern British Columbia: lidar, sunphotometry, and mountaintop chemistry observations. Atmospheric Chemistry and Physics 11, 465–477.

McMeeking, G.R., Kreidenweis, S.M., Baker, S., Carrico, C.M., Chow, J.C., Collett, J.L., Hao, W.M., Holden, A.S., Kirchstetter, T.W., Malm, W.C., Moosmüller, H., Sullivan, A.P., Wold, C.E., 2009. Emissions of trace gases and aerosols during the open combustion of biomass in the laboratory. Journal of Geophysical Research 114, D19210.

Müller, T., Laborde, M., Kassell, G., Wiedensohler, A., 2011. Design and performance of a three-wavelength LED-based total scatter and backscatter integrating nephelometer. Atmospheric Measurement Techniques 4, 1291–1303.

Real, E., Law, K.S., Weinzierl, B., Fiebig, M., Petzold, A., Wild, O., Methven, J., Arnold, S., Stohl, A., Huntrieser, H., Roiger, A., Schlager, H., Stewart, D., Avery, M., Sachse, G., Browell, E., Ferrare, R., Blake, D., 2007. Processes influencing ozone levels in Alaskan forest fire plumes during long-range transport over the North Atlantic. Journal of Geophysical Research 112, D10S41.

Reid, J.S., Koppmann, R., Eck, T.F., Eleuterio, D.P., 2005. A review of biomass burning emissions part II: intensive physical properties of biomass burning particles. Atmospheric Chemistry and Physics 5, 799–825.

Singh, H.B., Cai, C., Kaduwela, A., Weinheimer, A., Wisthaler, A., 2012. Interactions of fire emissions and urban pollution over California: ozone formation and air quality simulations. Atmospheric Environment 56, 45–51.

Weiss-Penzias, P., Jaffe, D., Swartzendruber, P., Hafner, W., Chand, D., Prestbo, E., 2007. Quantifying Asian and biomass burning sources of mercury using the Hg/CO ratio in pollution plumes observed at the Mount Bachelor Observatory. Atmospheric Environment 41, 4366–4379.

Weiss-Penzias, P., Jaffe, D.A., Swartzendruber, P., Dennison, J.B., Chand, D., Hafner, W., Prestbo, E., 2006. Observations of Asian air pollution in the free troposphere at Mount Bachelor Observatory during the spring of 2004. Journal of Geophysical Research 111, D10304.

Yokelson, R.J., Burling, I.R., Urbanski, S.P., Atlas, E.L., Adachi, K., Buseck, P.R., Wiedinmyer, C., Akagi, S.K., Toohey, D.W., Wold, C.E., 2011. Trace gas and particle emissions from open biomass burning in Mexico. Atmospheric Chemistry and Physics 11, 6787–6808.

Yokelson, R.J., Crounse, J.D., DeCarlo, P.F., Karl, T., Urbanski, S., Atlas, E., Campos, T., Shinozuka, Y., Kapustin, V., Clarke, A.D., Weinheimer, A., Knapp, D.J., Montzka, D.D., Holloway, J., Weibring, P., Flocke, F., Zheng, W., Toohey, D., Wennberg, P.O., Wiedinmyer, C., Mauldin, L., Fried, A., Richter, D., Walega, J., Jimenez, J.L., Adachi, K., Buseck, P.R., Hall, S.R., Shetter, R., 2009. Emissions from biomass burning in the Yucatan. Atmospheric Chemistry and Physics 9, 5785–5812.

Yokelson, R.J., Griffith, D.W.T., Ward, D.E., 1996. Open-path Fourier transform infrared studies of large-scale laboratory biomass fires. Journal of Geophysical Research 101, 21067–21080.